Shear-stress-induced phase transition in $KHCO_3$ studied by Brillouin scattering

Shigehiro Takasaka
Department of Physics, University of Tokyo, Tokyo 113-0033, Japan

Yuhji Tsujimi and Toshirou Yagi
Research Institute for Electronic Science, Hokkaido University, Sapporo 060-0812, Japan

(Received 28 November 2001; published 11 April 2002)

The XY shear stress σ_6' is applied to a single crystal of $KHCO_3$ and a pure transverse XY shear c_{66}' mode is observed by 90° Brillouin scattering in the VH scattering geometry, where X is the axis obtained by the rotation of the a^* axis around the b axis with 9° and Y is parallel to the b axis. A new phase induced by σ_6' is discovered from an anomalous softening behavior of the c_{66}' mode and is assigned to a ferrodistortive phase having an in-phase configuration of $(HCO_3)_2^-$ dimers. A phase diagram is successfully fabricated and is found to consist of three phases: the disordered, the antiferrodistortive, and the ferrodistortive phases. The triple point is determined to be a point ($T_{tr}=317.2\pm0.1$ K and $\sigma_{6tr}'=4.5\pm0.1$ kPa).

DOI: 10.1103/PhysRevB.65.174102 PACS number(s): 63.20.−e, 77.84.−s, 78.35.+c

I. INTRODUCTION

Potassium hydrogen carbonate $KHCO_3$ undergoes an antiferrodistortive phase transition of an order-disorder type at $T_N=318$ K under atmospheric pressure.[1–3] The space group is $C2/m$ (C_{2h}^3) in the high-temperature phase (phase I) and is $P2_1/a$ (C_{2h}^5) in the low-temperature phase (phase II).[1,4–7] The unique axis is the b axis in both phases. The crystal is composed of K^+ ions and $(HCO_3)_2^-$ dimers. Each dimer, a molecular unit of the order-disorder mechanism, is formed with two HCO_3 groups bounded by two hydrogen bonds. In phase I, dimers are disordered and each of them has two stable rotational angles around the c axis with the same probability as drawn in Fig. 1(a). In phase II, dimers are ordered with an antiphase configuration (Q_A configuration) as shown in Fig. 1(b). The order parameter of the phase transition is the order of the Q_A configuration of dimers.

It is natural to recognize that all anomalies related to the phase transition can be explained only by the softening of the relaxational antiphase dimer mode (Q_A mode). This recognition was, however, found to be wrong in the case of $KHCO_3$.[3] The softening behavior was discovered in the transverse acoustic c_{66} mode propagating along the a^* axis by ultrasonic and Brillouin scattering methods.[3,8] This behavior could not be explained at all by the softening of the Q_A mode, even if any order of coupling between the Q_A and the c_{66} modes is taken into account. Takasaka *et al.* introduced a new relaxational in-phase dimer mode (Q_F mode) and proved from space group considerations that the Q_F mode has to show the softening behavior toward T_N.[3] They concluded that the softening behavior of the c_{66} mode is caused by that of the Q_F mode through the bilinear coupling between them. Moreover, they confirmed the existence of the Q_F mode by Raman scattering experiment both in $KHCO_3$ and in deuterated compound $KDCO_3$.[9] Independently, Kakurai *et al.* found the existence of the Q_F mode in $KDCO_3$ by a thermal neutron spin-echo experiment.[2] They have reported that both the Q_A and Q_F modes soften simultaneously toward T_N with almost the same softening rate in phase I but the Q_A mode softens completely at T_N in advance of the Q_F mode. In this way, the antiferrodistortive phase appears under atmospheric pressure, instead of the ferrodistortive phase having an in-phase configuration (Q_F order) of dimers as shown in Fig. 1(c). It would be easily expected that the ferrodistortive phase will appear if one can assist the Q_F order of dimers by applying a conjugate force (F_{Q_F}) to the Q_F mode externally. Here the force F_{Q_F} is defined by $\partial G/\partial Q_F$

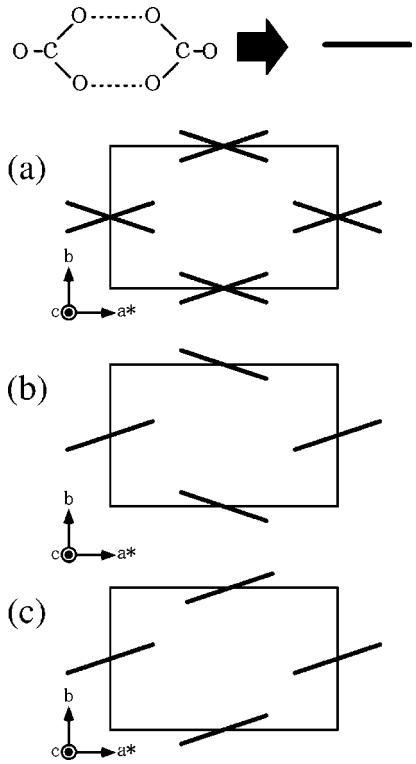

FIG. 1. Configuration of $(HCO_3)_2$ dimers on the c-plane projection. A dimer containing two hydrogen bonds (O - - - O) is represented by a thick solid line. A unit cell is designated by a rectangle. (a) Phase I with disordered configuration of dimers. (b) Phase II with antiferrodistortive Q_A configuration of dimers. (c) Phase with ferrodistortive Q_F configuration of dimers.

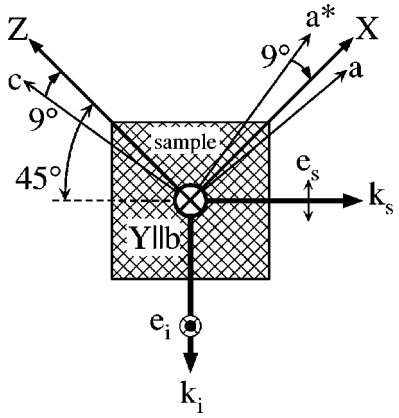

FIG. 2. Brillouin scattering geometry. The wave vectors $\mathbf{k}_i$ and $\mathbf{k}_s$ are those of the incident and scatted light, respectively. The incident light is vertically (**V**) polarized to the XZ scattering plane as indicated by $\mathbf{e}_i$ (⊗), and the scattered light is horizontally (**H**) polarized to the plane as indicated by $\mathbf{e}_s$ (↕). The c'_{66} mode propagates to the X axis with the displacement along the Y axis.

with a free energy G. Since F_{Q_F} cannot be applied directly, one must search an alternative external force working just as an effective conjugate force. The external XY shear stress σ'_6 is selected as the force in the present study, where X is the axis obtained by the rotation of the a^* axis around the b axis with 9° and Y is parallel to the b axis. It is apparent from space group considerations that $\sigma'_6=\partial G/\partial x'_6$ is proportional to $F_{Q_F}=\partial G/\partial Q_F$ through the bilinear coupling between the XY shear strain x'_6 and Q_F in both phases I and II. Therefore, the external stress σ'_6 can be the effective conjugate force we search. On the other hand, the c'_{66} mode associated with x'_6 was chosen here as a best probe for the detection of the phase transition because this mode has been reported to show the strongest softening behavior of all pure transverse acoustic modes which couple bilinearly to the Q_F mode.[10] The special selection of σ'_6 described above is closely related to the fact that σ'_6 is a conjugate force to this c'_{66} mode.

The purpose of this paper is to induce the ferrodistortive phase by application of σ'_6 and to make up the phase diagram of $KHCO_3$ at the same time. For this purpose, the softening behavior of the c'_{66} mode under σ'_6 shear stress is carefully investigated by a 90° Brillouin scattering experiment.

II. EXPERIMENT

A single crystal of $KHCO_3$ was grown by slow cooling (about 0.2 K/day) from a saturated aqueous solution filtered with a microfilter of 0.2 μm pore size. A prism-shapel sample of size $3\times5\times3$ mm^3, the edges of which are parallel to $X-Z$, Y, and $X+Z$, respectively, was cut out from a grown crystal by being referred to the dominant cleavage plane $(40\bar{1})$ and the natural rectangular plane (100). Here we introduced a new Cartesian coordinate system with the axes (X, Y, and Z) as shown in Fig. 2, where X and Z are the axes obtained by rotation of the a^* and c axes, respectively, around the b axis with 9°, and Y is parallel to the b axis.[10]

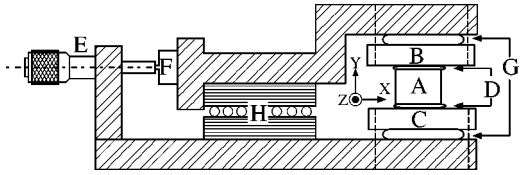

FIG. 3. Sample cell for applying the σ'_6 shear stress. A: sample. B: top plate. C: bottom plate. D: elastic adhesive. E: micrometer. F: stress sensor. G: Péltier devices. H: sliders.

After the surfaces of the sample were polished carefully for reduction of the scattered light from the surfaces, the sample was set in a homemade sample cell designed for applying only the XY shear stress σ'_6 to the sample. The side elevation view of the cell is shown in Fig. 3. The sample is bonded between two aluminum plates, the top plate and the bottom plate, with elastic adhesive (Cemedine EP001) made of an epoxy resin. The top plate can move to only one direction parallel to the surface of the fixed bottom plate by a micrometer. The X axis of the sample was set parallel to this movable direction, and the Y axis was set perpendicular to the surfaces of the both plates, which enables us to apply only the σ'_6 shear stress to the sample. The magnitude of σ'_6 was measured by a stress sensor (KYOWA LM-100KA) within an error of ±0.1 kPa. It is worth emphasizing that the applied stress is properly transferred to the sample through adhesive. We carefully selected a soft and elastic adhesive with quick response to the applied stress. Moreover, the applied stress is up to only 6–7 kPa in our experiment. Under these conditions, it is plausible that the adhesive behaves like a spring. When a stress gradient is caused inside the adhesive by some reasons, the adhesive behaves like a spring and changes its form to remove this gradient quickly. As a result, the stress at the sample position becomes equal to the applied stress. The temperature of the sample cell was controlled by two Péltier devices fastened to each aluminum plate and was stabilized by a temperature stabilizer (Ohkura EC5700). The temperature of the sample was measured by a thermocouple attached to the sample and was found to have stability within ±0.02 K.

The 90° Brillouin scattering experiment was performed in the VH scattering geometry $[-X-Z(Y,X+Z)X-Z]$ as drawn in Fig. 2. The crystal symmetry of $KHCO_3$ is monoclinic in phases I and II. Taking the optical indicatrix into account,[11–13] one should carefully identify the acoustic mode observed in this geometry. Since one of the optical axes is parallel to the Y axis, the incident beam with **V** ($\|Y$) polarization enters straight into the sample, keeping its polarization. Another optical axis lies in the XZ plane and makes an angle of 6° to X-Z. We estimated from the reported values of refractive indices that the scattered beam, coming out of the sample along X-Z with **H** ($\|X+Z$) polarization, runs inside the sample along the direction making an angle of about 1° to X-Z in the XZ plane with the same **H** polarization. Thus, the pure transverse c'_{66} mode propagating to the X axis with the displacement along the Y axis is surely observed in our scattering geometry within an error of 0.5/90 (half of the error of the scattering angle 1/90). Although this estimation is based on the refractive indices measured at room tempera-

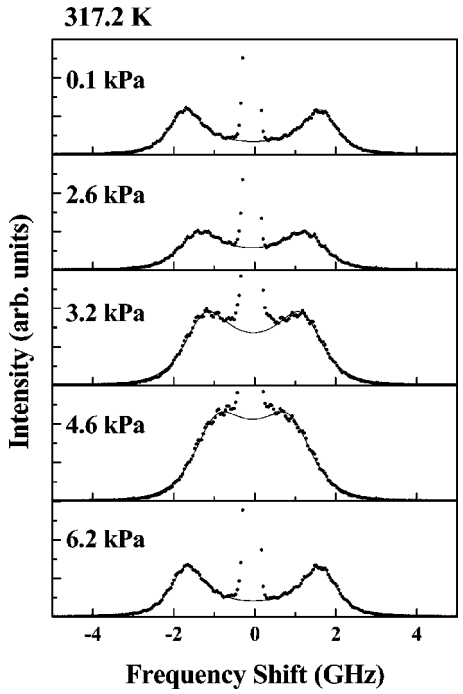

FIG. 4. Typical Brillouin scattering spectra of the c'_{66} mode observed under several stresses σ'_6 at 317.2 K. Each thin line indicates a least-squares fit with a damped-harmonic oscillator function.

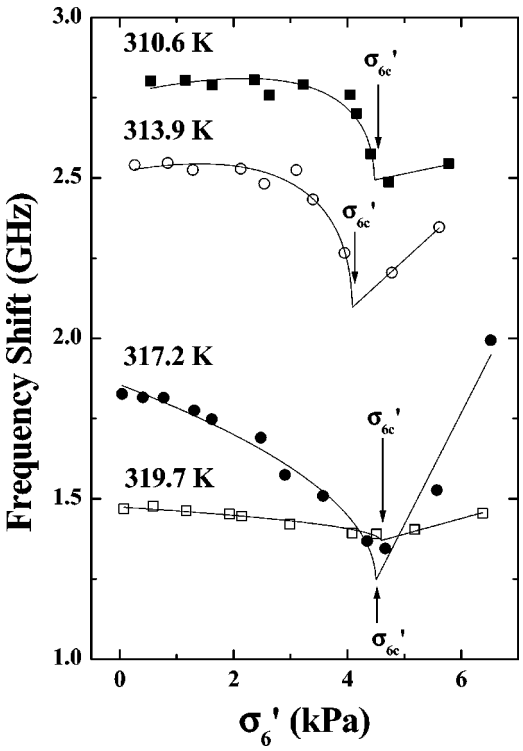

FIG. 5. The σ'_6 shear stress dependence of the frequency shift $\Delta\nu$ of the c'_{66} mode observed at the temperatures $T=310.6$, 313.9, 317.2, and 319.7 K. Each thin line indicates a least-squares fit of the obtained $\Delta\nu$ data to an empirical fitting function $A_1|\sigma'_6-\sigma'_{6c}| + B_2\sqrt{|\sigma'_6-\sigma'_{6c}|}$.

ture under atmospheric pressure, the estimation is considered to be valid over the temperature and applied stress ranges covered in our experiment for the following reasons: the optical indicatrices are intrinsically identical in phases I and II under atmospheric pressure[14] and the dependence of the optical indicatrix on the applied stress is expected to be very small, because the stress is up to only 6–7 kPa.

As a light source, a longitudinal single mode Ar^+ laser (Spectra-Physics BeamLok 2060 with Z-Lok and J-Lok) was used with a power of 200 mW at a wavelength of 514.5 nm. The power fluctuation was stabilized within ± 1 mW by the Jitter-Lock mechanism of the laser. The scattered light from the sample was collected and was examined by a 3+3 pass tandem Fabry-Perot interferometer of Sandercock type. The free spectral range was set to be 10 GHz and a resolution more than 0.05 GHz was achieved. The examined light was detected by a photomultiplier (Hamamatsu R585) and was stored in the memory of a multichannel analyzer as a spectrum after 1000 times accumulation. The Brillouin peak caused by the c'_{66} mode was analyzed by the fit with a damped harmonic oscillator function so as to obtain the frequency shift $\Delta\nu$ of the peak.

III. RESULTS AND DISCUSSION

In order to find a ferrodistortive phase, the σ'_6 shear stress is applied to the sample and the c'_{66} mode is investigated by the 90° Brillouin scattering experiment in the *VH* scattering geometry. The σ'_6 shear stress dependence of the Brillouin spectrum was studied at fixed temperature. Figure 4 shows the typical Brillouin spectra of the c'_{66} mode obtained at $T=317.2$ K. The anomalous softening behavior is clearly seen and the Brillouin doublet almost overlaps with the Rayleigh peak at $\sigma'_6=4.6$ kPa. Figure 5 shows the frequency shift $\Delta\nu$ of the c'_{66} mode as a function of σ'_6 at the four fixed temperatures. Concentrating on the data at $T=317.2$ K, we fit the obtained $\Delta\nu$ data to an empirical fitting function of $A_1|\sigma'_6-\sigma'_{6c}|+B_2\sqrt{|\sigma'_6-\sigma'_{6c}|}$ with fit parameters A_1, B_1, and σ'_{6c}. One can calculate the σ'_6 dependence of $\Delta\nu$ from the free energy G and the refractive indices in principle. However, the calculated results are too complicated to be handled. Here only an estimation of σ'_{6c} is important, but the precise discussion about the stress dependence of $\Delta\nu$ is not needed. This is the reason why we used the empirical fitting function. It was found from the fit that $\Delta\nu$ takes a minimum value of 1.35 ± 0.05 GHz at $\sigma'_{6c}=4.5\pm0.1$ kPa. This indicates that a new phase transition takes place at the critical shear stress σ'_{6c} and a new phase appears above σ'_{6c} at $T=317.2$ K. Hereafter, this newly found phase will be called phase III. We can also determine σ'_{6c} from Fig. 5 to be 4.5 ± 0.1, 4.1 ± 0.1, and 4.6 ± 0.1 kPa at $T=310.6$, $T=313.9$, and $T=319.7$ K, respectively. The same experiment was performed repeatedly at each of the 23 different fixed temperatures in order to determine the phase boundary of phase III (phase boundary A). The critical shear stress σ'_6 obtained at each temperature is plotted in Fig. 6 by an open circle. The phase boundary A is successfully determined by a sequence of open circles. It will be concluded later that phase III is a

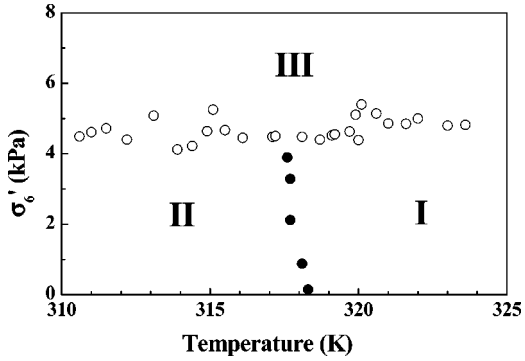

FIG. 6. Phase diagram of $KHCO_3$. The open circles, which are the critical stresses σ'_{6c} determined at the 27 different fixed temperatures, form a phase boundary A. The solid circles, which are the critical temperatures T_c determined under the 5 different almost-fixed σ'_{6c} shear stresses, form a phase boundary B. Phases I, II, and III are identified to be the disordered phase, the antiferrodistortive phase, and the ferrodistortive phase, respectively.

ferrodistortive phase having an in-phase configuration (Q_F order) of dimers.

It has been already established that the antiferrodistortive phase transition occurs at the critical point ($T_N=318$ K, $\sigma'_6=0$ kPa).[1–3] This fact implies the existence of other phase boundary (phase boundary B), starting from this critical point and ending at a triple point on phase boundary A. In order to determine phase boundary B, the temperature dependence of the Brillouin scattering spectrum was investigated under almost fixed shear stress σ'_6. It was very difficult to keep the stress constant due to the thermal expansion of the sample. The measured stress has a temperature dependence of about 0.1 kPa/K. For this reason, the value of σ'_6 given in this paragraph means the value measured at the critical temperature T_c determined later. Figure 7 shows the typical temperature dependence of the Brillouin spectra of the c'_{66} mode measured at $\sigma'_6=3.9$ kPa. The anomalous softening behavior is clearly seen in this figure. Figure 8 shows the typical temperature dependence of the frequency shift of the c'_{66} mode measured under each of the shear stresses $\sigma'_6=0.1$,2.1, and 3.9 kPa. Fitting the obtained $\Delta\nu$ data to an empirical fitting function of $A_2|T-T_c|+B_2\sqrt{|T-T_c|}$ with fit parameters A_1, B_2, and T_c, we find that $\Delta\nu$ takes a minimum value of 1.44 ± 0.05 GHz (at $T_c=318.4\pm0.1$ K under $\sigma'_6=0.1$ kPa), 1.50 ± 0.05 GHz (at $T_c=317.8\pm0.1$ K under $\sigma'_6=2.1$ kPa), and 1.28 ± 0.05 GHz (at $T_c=317.7\pm0.1$ K under $\sigma'_6=3.9$ kPa), respectively. The parameter T_c can be assigned to the critical temperature. The same experiment was performed also under $\sigma'_6=0.9$ kPa and $\sigma'_6=3.3$ kPa. The critical temperatures determined in the present experiment are plotted with solid circles in Fig. 6. The sequence of solid circles represents the phase boundary B. The high- and low-temperature phases divided by this boundary are redefined as phases I and II, respectively. The triple point is determined to be ($T_{tr}=317.2\pm0.1$ K, $\sigma'_{6tr}=4.5\pm0.1$ kPa) from the intersection of two phase boundaries A and B.

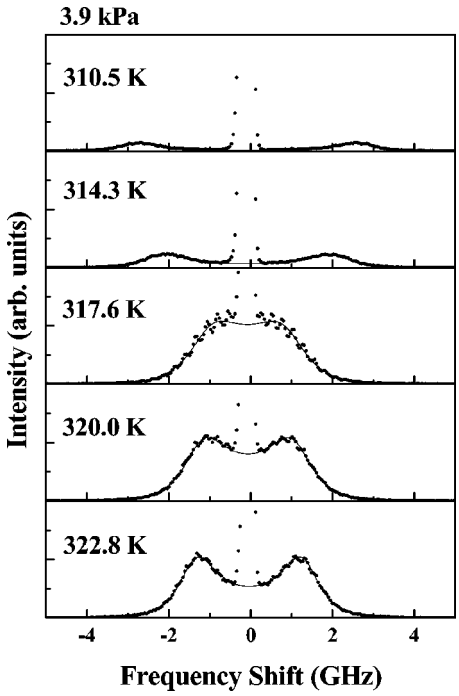

FIG. 7. Typical Brillouin scattering spectra of the c'_{66} mode obtained at several temperatures under $\sigma'_6=3.9$ kPa. Each thin line indicates a least-squares fit with a damped-harmonic oscillator function.

Phases I and II can be identified to be the disordered and the antiferrodistortive phases, respectively, because of the phase continuity from the phases under atmospheric pressure. For the identification of phase III, the existence of domains in phase II gave us an idea. When the incident laser

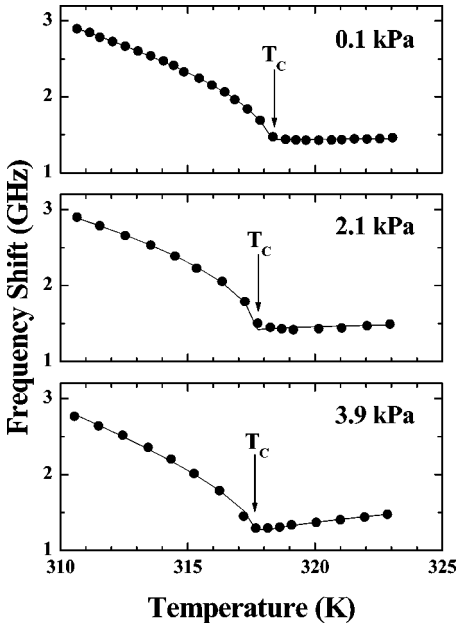

FIG. 8. Temperature dependence of the frequency shift $\Delta\nu$ of the c'_{66} mode measured under the shear stresses $\sigma'_6=0.1$, 2.1, and 3.9 kPa. Each thin line indicates a least-squares fit of the obtained $\Delta\nu$ data to an empirical fitting function $A_2|T-T_c|+B_2\sqrt{|T-T_c|}$.

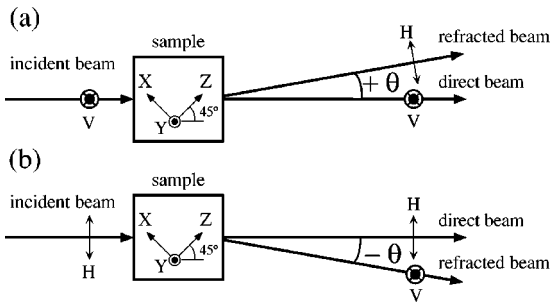

FIG. 9. Schematic illustration of the refracted beams and their polarizations. θ is the angle between the direct and refracted beams. Symbols ⊙ and ↕ placed on the beams represent the **V** and **H** polarizations, respectively.

beam passes through the sample under the external shear stress σ_6' in phase II, a refracted laser beam appears together with a direct beam as shown in Fig. 9. When the incident beam has **V** polarization, the refracted beam with **H** polarization is emitted at the angle of $\theta = +5.8° \pm 0.2°$ with the direct beam as shown in Fig. 9(a). In the case of the incident beam with H polarization, the refracted beam with V polarization is emitted at $\theta = -5.8° \pm 0.2°$ with the direct beam as shown in Fig. 9(b). The angle θ is almost independent of temperature and of the shear stress σ_6'. The refracted beams completely disappear in phases I and III. These phenomena are clearly not due to birefringence. Since one of the optical axes is parallel to the Y axis, the incident beam with **V** ($\|Y$) or **H** ($\|X+Z$) polarization has to run in the sample as one beam with the same polarization. The splitting of the incident beam into two beams cannot be explained at all by birefringence. The authors have already found these phenomena under the external shear stress σ_6 and have understood these phenomena as follows.[15] There are two series of domains in phase II, refractive indices of which differ from each other, and some part of the incident beam is refracted by the domain boundary due to the change of the refractive indices as in the cases of both ferroelastic crystals $Gd_2(MoO_4)_3$ and $Bi_4Ti_3O_{12}$.[16] Grand *et al.* have performed a more precise light refraction experiment and observed the same refraction phenomena even under atmospheric pressure in their as-grown crystal.[14] They explained completely the refraction phenomena by the existence of ferroelastic domains in the antiferrodistortive phase below T_N. Their explanation is based on the x-ray results reported by Kerst that the triclinic ferroelastic domains (space group $C1$ or $C\bar{1}$) can be induced when the uniaxial pressure is applied to the sample below T_N.[7]

The existence of domains was also confirmed in the present experiment by another way, that is, by observation of a laser beam path in the sample. When the external shear stress σ_6' is applied to the sample, glittering points begin to appear along the beam path. The points are found to appear only under σ_6' and only in the region of phase II except near phase boundaries A and B. At any temperature in this region, the number of glittering points increases with an increase in σ_6' up to about a half of the critical stress $\sigma_{6c}'/2$ and decreases with a further increase in σ_6'. This phenomenon can be naturally explained if we suppose that the domains are the regions of phase III. Since the points always appear at the same position, the physical origin should be lattice defects. When σ_6' is applied externally to the sample, a stress concentration takes place around defects. If the local stress around the defect exceeds σ_{6c}', the region of phase III can appear in phase II as a domain making a glittering point in the laser beam path. This is quite reasonable because σ_{6c}' is only 4–5 kPa (one can produce this amount of shear even by two fingers) as known from Fig. 6. As σ_6' increases, the number of defects with local stress in excess of σ_{6c}' is expected to increase. This is the reason why the number of glittering points increases with the increase in σ_6' up to $\sigma_{6c}'/2$. On the other hand, the movement of the $(HCO_3)_2^-$ dimers, which are the molecular units of the order-disorder mechanism, plays an important role above $\sigma_{6c}'/2$, because phase III will be assigned later to be the ferrodistortive phase having an in-phase configuration (Q_F order) of dimers. The dimers, inclusive of the dimers around defects, can move easily near phase boundaries A and B, because the fluctuation of dimer's orientation increases drastically near the critical point. In other words, not only phase II but also the domains of phase III become unstable near phase boundaries A and B. This obscures the domain boundary and the number of glittering points decreases with the further increase in σ_6' from $\sigma_{6c}'/2$ as a result. In this way, the existence of domain can be naturally explained when we presume that the domain is the region of phase III induced by the local stress around defects in antiferrodistortive phase II.

As mentioned above, Kerst have reported that the domain is the region of ferroelastic phase with a space group $C1$ or $C\bar{1}$.[7] On the other hand, it is apparent from Fig. 3 drawn in the report of Grand *et al.* that this ferroelastic phase has a spontaneous shear strain x_{6s}'.[14] Taking their reports and our presumption described above (the domain is the region of phase III) into account, we can predict that phase III is the ferroelastic phase with x_{6s}'. This ferroelastic phase must have a spontaneous in-phase configuration (Q_F order) of dimers [see Fig. 1(c)], because the shear strain x_6' can couple bilinearly to Q_F under $C1$ or $C\bar{1}$ space group symmetry. Furthermore, it has been already proved by the present authors that the phase with the Q_F order—that is, the ferrodistortive phase-must have a space group $P\bar{1}$ ($C\bar{1}$ in a nonstandard setting).[3] These considerations lead us to the final conclusion that phase III is a ferrodistortive phase with Q_F and is also a ferroelastic phase with x_{6s}', and its space group is $P\bar{1}$.

At the end of this paper, we reconsider the statement by Grand *et al.* that the crystal exhibits two structural phase transitions (an antiferrodistortive and a ferroelastic phase transition) that take place at nearly the same critical temperature (T_N).[14] This statement may lack accuracy from the viewpoint of our present experimental results. Real ferrodistortive (ferroelastic) and real antiferrodistortive phase transitions occur on phase boundaries A and B, respectively, as shown in Fig. 6. Nevertheless, the region having ferrodistortive (ferroelastic) order can coexist as domains only in the antiferrodistortive phase II. The coexistence disappears to-

gether with the disappearance of phase II at almost constant critical temperature T_c ($\approx T_N$) on phase boundary B, which probably led their inaccurate statement.

IV. SUMMARY

A ferrodistortive phase having an in-phase configuration (Q_F order) of $(HCO_3)_2^-$ dimers can be successfully induced by the external shear stress σ_6'. A phase diagram is fabricated from the study of the softening behavior of the c_{66}' mode observed by the 90° Brillouin scattering experiment in VH scattering geometry under σ_6'. The diagram consists of three phases: the disordered, the antiferrodistortive, and ferrodistortive phases. The triple point is determined to be a point ($T_{tr}=317.2\pm0.1$ K, $\sigma_{6tr}'=4.5\pm0.1$ kPa).

ACKNOWLEDGMENT

The present work has been supported in part by a Grant-in-Aid for Scientific Research from the Ministry of Education, Science, Sports and Culture of Japan, No. 12640365 and No. 11874054.

[1] S. Kashida and K. Yamamoto, J. Solid State Chem. **86**, 180 (1990).
[2] K. Kakurai, T. Sakaguchi, M. Nishi, S. Kashida, and Y. Yamada, Phys. Rev. B **53**, 5974 (1996).
[3] S. Takasaka, Y. Tsujimi, and T. Yagi, Phys. Rev. B **36**, 10 715 (1997).
[4] I. Nitta, Y. Tomiie, and C.H. Koo, Acta Crystallogr. **5**, 292 (1952).
[5] J.O. Thomas, R. Tellgren, and I. Olovsson, Acta Crystallogr., Sect. B: Struct. Crystallogr. Cryst. Chem. **30**, 1155 (1974).
[6] M. Machida, Y. Yamaguchi, M. Sugiyama, Y. Iwata, N. Koyano, and S. Fukui, Physica B **213-214**, 393 (1995).
[7] H. Kerst, Ph.D. thesis, Institute für Kristallographie, Aachen, 1995.
[8] S. Haussühl, Solid State Commun. **57**, 643 (1986).
[9] S. Takasaka, Y. Tsujimi, and T. Yagi, J. Korean Phys. Soc. **29**, S444 (1996).
[10] S. Takasaka, Y. Tsujimi, and T. Yagi, Ferroelectrics **203**, 167 (1997).
[11] Landolt-Börnstein, edited by J. Bartels, H. Borchers, H. Hausen, K.-H. Helwege, K.L. Schäfter, and E. Schmiot, Vol. 2, Part 8, p. 2-56 (Springer-Verlag, Heidelberg, 1962).
[12] J. Fousek and J. Petzelt, Phys. Status Solidi A **55**, 11 (1979).
[13] W.H. Miller, Poggendorffs Ann. Physik **55**, 628 (1842).
[14] Y.L. Grand, D. Rouede, J. Wienold, and J. Glinnemann, J. Phys. Soc. Jpn. **67**, 1451 (1998).
[15] S. Takasaka, Y. Tsujimi, and T. Yagi, J. Korean Phys. Soc. **32**, S565 (1998).
[16] T. Tsukamoto, J. Hatano, and H. Futama, J. Phys. Soc. Jpn. **53**, 838 (1984).